




Cite this: *Analyst*, 2025, **150**, 3578

## Screening and classification of hydrogenated vegetable oils using a combination of SFC-FID, SFC-MS and GCxGC-MS†

Laval R. Nicolas, <sup>a</sup> Jim Barker,<sup>b</sup> Jody Clark,<sup>c</sup> G. John Langley<sup>a</sup> and Julie M. Herniman<sup>\*a</sup>

This study employs a combination of orthogonal chromatographic and detection techniques to screen and characterise hydrogenated vegetable oils (HVOs), addressing the question of whether HVOs share the same composition. The data revealed that the HVOs are different, and the variations are primarily influenced by the initial feedstocks and production processes. Significant variations in linear and branched hydrocarbon distribution, particularly in the C14–C18 range were observed and the detection of polar components, such as free fatty acids, fatty acid methyl esters, and *mono*-, *di*-, and *tri*-acylglycerides in some samples, suggested potential concerns related to fuel storage, delivery, and performance. Each analytical technique contributed unique insights: GCxGC-MS provided extended chromatographic resolution and detailed identification of saturates and aromatics, including the critical *iso*-alkane to *n*-alkane ratio, which is essential for predicting cold flow properties. Additionally, a streamlined data visualisation method was introduced to facilitate the assessment of fuel profile. SFC-FID enabled quantitative group-based separations of polars, saturates, and aromatics with minimal sample preparation and SFC-ESI-MS selectively separated and detected individual polar compounds. The combined approach highlights the importance of using multiple techniques to obtain a chemical profile of the individual HVOs. Given the observed compositional differences, this study suggests that “HVO” is an overly broad term that does not accurately reflect the chemical diversity of these fuels. A refined classification system distinguishing HVO subclasses is suggested that better represents these variations.

Received 15th April 2025,

Accepted 5th July 2025

DOI: 10.1039/d5an00429b

rsc.li/analyst

## Introduction

Hydrogenated vegetable oils (HVOs) or green diesels are the latest generation of biodiesel, typically manufactured by the catalytic hydrogenation of triacylglycerides (TAGs), that are typically sourced from edible and non-edible feedstocks, and can include waste oil/fat streams.<sup>1,2</sup> Whilst not restricted to TAGs specifically, HVOs can be manufactured using existing hydrotreatment infrastructures that are employed for the removal of sulfur and other upgrading processes in petroleum products.<sup>3,4</sup> Fig. 1 shows a simplified representation of the reactions that take place during hydrotreatment. Unsaturated bonds along the fatty acid chains undergo catalytic hydrogenation (Fig. 1, rxn 1), followed by the liberation of the free fatty

acids (FFAs) from the glycerol backbone. Once liberated, the FFAs can undergo three possible, competing reaction pathways: decarboxylation (rxn 3), hydrodecarbonylation (rxn 4), and hydrodeoxygenation (rxn 5).<sup>5–7</sup> The final product is a paraffinic hydrocarbon mixture, low in heteroatom content and can be used as produced or as a drop-in fuel for compression ignition engines. The properties of the manufactured HVO, for a given feedstock, are largely dependent upon the reaction conditions and the catalysts used. Additionally, secondary processes, such as catalytic hydroisomerisation and hydrocracking (rxn 6 and 7 respectively), may be employed to enhance the low temperature properties of the fuel.<sup>2,5,8</sup>

Herein lies the challenge of analysing HVOs, where there is a broad variety of feedstocks, catalysts, reaction conditions and manufacturing processes. The work described here uses multiple orthogonal chromatography and detection techniques to identify similarities and differences in these complex new renewable diesel fuels.

Supercritical fluid chromatography – flame ionisation detection (SFC-FID) is a technique that uses a mobile phase comprised of 100% supercritical carbon dioxide (scCO<sub>2</sub>) and

<sup>a</sup>School of Chemistry and Chemical Engineering, University of Southampton, SO17 1BJ, UK. E-mail: J.M.Herniman@soton.ac.uk

<sup>b</sup>Innospec Limited, Ellesmere Port, CH65 4EY, UK

<sup>c</sup>Selerity Technologies Inc., Salt Lake City, Utah, USA

† Electronic supplementary information (ESI) available. See DOI: <https://doi.org/10.1039/d5an00429b>





Fig. 1 Simplified reaction scheme for the production of HVOs from triacylglycerides.

packed columns, connected to two sets of switching valves. The solvent strength of  $\text{scCO}_2$  is similar to hexane and has the properties of both a gas and a liquid.<sup>9</sup> Its chromatographic property can be modified by changing the pressure or the temperature of the system.

A unique feature of the SFC-FID instrumentation is the ability to trap, isolate and control the direction of flow of the mobile phase through the columns, and this is used in the standard method ASTM D5186 for the determination of aromatic and polyaromatic content in aviation and diesel fuels.<sup>10</sup> This analysis is a group-type separation of the saturated alkane, aromatic, and polar content of the sample and should be an appropriate approach for the analysis of HVOs. The FID can be considered as a near-universal detector and so can offer a rapid means to quantitatively determine the composition of a fuel *via* this group-type separation. Whilst 1D-GC-MS has been used successfully for analysis of fuels, significant co-elution is often observed, even with extended analysis times, and advanced data treatment/sample preparation is still required.<sup>11–13</sup> The high peak capacity, resolution, and versatility of comprehensive two-dimensional gas chromatography – mass spectrometry (GCxGC-MS) overcomes this and has proven to be effective for the analysis of complex samples such as petroleum based fuels, and again aligns well with the requirements for analysis of HVO.<sup>14–18</sup> Vendevre *et al.* demon-

strated the capability of the technique to obtain a repeatable pattern of components eluting in regions based on chemical functionality.<sup>19</sup>

Gough and Langley exploited the strength of ESI-MS for the analysis of corrosion inhibitors in fuels and oils, utilising the selectivity of ionisation of polar species and rendering the non-ionisable compounds invisible, reducing interference in the mass spectra.<sup>20</sup> Hyphenating packed column SFC, used with modifiers and additives, coupled to ESI-MS adds the selectivity of the chromatography to the selective ionisation of polar species present that were found in previous fuels derived from plant materials, *e.g.*, FFAs, TAGs, diacylglycerides (DAGs) and monoacylglycerides (MAGs), all precursor components used in HVOs.<sup>21–23</sup>

Each of these techniques provides orthogonal yet overlapping information with varying levels of granularity. SFC-FID group-type analysis offers a straightforward composition breakdown into saturated, aromatic, and polar content based on FID response from an undiluted fuel injection. However, a key limitation of SFC-FID is its inability to provide detailed structural information. GCxGC-MS provides a signature of the volatile and semi-volatile fuel components, classifying analytes by chemical functionality. However, it is insufficient for fully characterising the HVOs, particularly when analysing some polar, thermally labile, or non-volatile components of the fuel. To address this limitation, SFC-ESI-MS allows for selective ionisation of polar molecules whilst minimising interferences from the fuel matrix.

In this study, the three techniques were employed in parallel to typify seven unknown HVO fuel samples and answer the initial question ‘are all HVOs the same?’. Every sample was analysed using each individual technique, and following screening of the data, in-depth data analysis was directed by the initial findings. For example, when polar content was observed in any of the techniques then more detailed interrogation of the SFC-MS data was undertaken to identify these individual species.

## Experimental

### Samples and reagents

Methanol (liquid chromatography – mass spectrometry (LC-MS) grade), dichloromethane (DCM, high performance liquid chromatography (HPLC grade)) was purchased from Thermo-Fisher Scientific (Loughborough, UK) and ammonium acetate ( $\text{NH}_4\text{OAc}$ , reagent grade) was purchased from VWR International (Lutterworth, UK). The seven HVO samples were supplied by Innospec Ltd (Ellesmere Port, UK). Throughout this study the samples were diluted using DCM in a ratio of 1 : 100 or analysed neat (undiluted).

### Two-dimensional gas chromatography – time of flight mass spectrometry (GCxGC-MS)

A LECO Pegasus BT 4D GCxGC-TOFMS (LECO Corp., St Joseph, MI, USA) equipped with an OPTIC multimode inlet



system and PAL3 autosampler was used for all 2D GC-MS analyses. The first-dimension column was a Rxi-5SilMS capillary column (Restek, 30 m × 0.25 mm inner diameter, 0.25 μm film thickness) and the second-dimension column was a Rxi-17SilMS capillary column (Restek, 1.3 m × 0.25 mm inner diameter, 0.25 μm film thickness). The inlet system was set at a constant temperature of 280 °C and held at this temperature until the end of the chromatography run time. Helium was used as the carrier gas at a constant flow rate of 1 mL min<sup>-1</sup>. The samples were analysed using a split ratio of 450 : 1 with a 0.2 μL injection volume. The oven temperature program used for the analysis had an initial temperature of 40 °C, increased at 4 °C min<sup>-1</sup> to 300 °C and held for 2 minutes. The data were acquired and processed using the LECO ChromaTOF BT software suite (version 5.55.35). The software controlling the PAL system was PAL Sample Control (version 3.1), and the OPTIC was controlled using Evolution Workshop 4 software.

The modulator temperature offset was set to +15 °C and the second oven offset was set to +5 °C with respect to the first oven. The modulator was a two-stage liquid nitrogen thermal modulator, with a modulation time of 5 seconds.

70 eV EI mass spectra were collected over a *m/z* range 35–550 at an acquisition rate of 200 spectra per second and an extraction frequency of 30 kHz. Analytes were identified by referencing their mass spectra to the National Institute of Standards and Technology (NIST) EI mass spectra library. The dataset was limited to the peaks with signal-to-noise of greater than 100, and the peak area response was obtained from the total ion current (TIC).

### Supercritical fluid chromatography – mass spectrometry (SFC-MS)

The diluted samples were analysed using a Waters ACQUITY UPC2™ coupled to a SQD2 (Waters Corp., Milford, MA, USA). Supercritical carbon dioxide (scCO<sub>2</sub>) was used as the mobile phase with a co-solvent of 25 mM NH<sub>4</sub>OAc in methanol. A Waters BEH column (100 mm × 3.0 mm, particle size 1.7 μm) was used, kept at a constant temperature of 40 °C and the system back pressure was set to 105 bar. The mobile phase flow rate was 1.5 mL min<sup>-1</sup>, and 5 μL of sample was injected. The solvent gradient started at 100% scCO<sub>2</sub>, the amount of co-solvent was increased from 0% to 1% over 3 minutes and then from 1% to 5% over 1.5 minutes. The co-solvent was increased again from 5% to 40% over 9 minutes. The make-up solvent flow rate was delivered at 0.45 mL min<sup>-1</sup> of 25 μM NH<sub>4</sub>OAc in methanol throughout the analysis.

The positive and negative ion electrospray ionisation (ESI) mass spectra were recorded using MassLynx™ software (version 4.1). The ionisation conditions were as follows: capillary voltage, 3.0 kV; cone voltage, 25.0 V; extractor, 3.0 V; source temperature, 150 °C; desolvation temperature, 500 °C; and desolvation gas flow, 550 L h<sup>-1</sup>, scan *m/z* range 85 to 1200 with a scan duration of 0.2 s.

### Supercritical fluid chromatography – flame ionisation detection (SFC-FID)

The undiluted samples were analysed using a 4000 Series SFC-FID and the packed columns were supplied by Selerity

Technologies, Inc (Salt Lake City, UT, USA). Column 1 was a bare silica (50 mm × 4.6 mm, particle size 5 μm) and column 2 was a bare silica (500 mm × 4.6 mm, particle size 5 μm) connected in series by two six-way valves (Valves A and B). The analysis used 100% scCO<sub>2</sub> as the mobile phase at a constant temperature of 40 °C and constant pressure of 200 bar. On injection, valve A is in the 'ON' position for 1.5 minutes, then the valve is switched into the 'OFF' position for 6.5 minutes. At 8 minutes, valve A is switched back to the position 'ON' position for the duration of 22 minutes.

The FID conditions were as follows: detector temperature, 400 °C; hydrogen flow rate, 27 Arb (arbitrary units); airflow rate, 12 Arb; range, 10 V and a detector frequency, 10 Hz.

## Results and discussion

### Screening of geographically different HVOs

Seven separate HVO were sourced from different geographic regions and analysed by the three different chromatographic techniques. Critical information required is the purity of the hydrocarbon mixture, *iso*-alkane to *n*-alkane ratio (linked to cold flow property), and identification of any other species present. For the screening, a uniform ionisation response for close homologues and isomers has been assumed to be the same. Similarly, it was assumed that the transfer of compounds from the GC inlet onto the GC column is uniform for all compounds.

The GCxGC-MS analysis of HVO 1 (Fig. 2) revealed the major component of the fuel to be paraffins. Note, with a non-polar column in the first dimension and a polar column in the second dimension the paraffinic species elute first in the second dimension. Further, the paraffinic species are separated and identified as *iso*-alkanes and *n*-alkanes. The first dimension of separation is closely related to the boiling point of the hydrocarbons, as the number of carbon atoms increases, the retention in the first dimension increases, with the *iso*-alkanes generally having a lower boiling point compared to the *n*-alkane.<sup>24</sup> The carbon number distribution of the HVO was



Fig. 2 Two-dimensional total ion current chromatogram (TICC) contour plot of the GCxGC-MS analysis of diluted HVO 1.



heavily weighted towards alkanes with 15–18 carbon atoms, this could indicate the type of feedstock used in the manufacture of the HVO. This aligns with data from the Food and Agriculture Organisation of the United Nations, where they state that the top four most readily produced vegetable oils are palm, soybean, rapeseed, and sunflower respectively.<sup>25</sup>

Fig. 2 shows the elution order of the *n*-alkanes (annotated with the number of carbon atoms, *e.g.*, *n*-C18 being *n*-octadecane). The red regions in the contour plot are related to intensity of signal, indicating higher concentrations of the different species in the fuel. For HVO 1 the C18 alkanes are the most abundant. The high abundance of the odd numbered carbon chain alkanes, C15 and C17 hydrocarbons suggests a decarboxylation process has occurred to remove the heteroatom because pentadecanoic acid (C15:0) and heptadecanoic acid (C17:0) fatty acids are only present as minor components in vegetable oils.<sup>26–28</sup> The hydrotreatment of the feedstock results in a significant amount of decarboxylation and decarbonylation reactions taking place, leading to the loss of a carbon atom from the FFA backbone. This suggests that the initial feedstocks were canola or rapeseed oils.<sup>29–31</sup>



Fig. 3 Two-dimensional TICC contour plot of the GCxGC-MS analysis of HVO 2-diluted.



Fig. 4 GCxGC-MS TICC contour plot of HVO 3-diluted (left). Note: overloading observed in the second dimension. 70 eV EI-MS and NIST 2017 library match of hexadecanoic acid (C16:0) detected in the sample (right).

The contour plot shown in Fig. 3 of a second HVO, HVO 2 is very similar to the contour plot for HVO 1 in paraffinic content, *i.e.*, *n*-alkanes and *iso*-alkanes, though some very subtle differences in specific *iso*-alkanes present can be seen.<sup>27,28</sup> These data suggest catalytic isomerisation was used to improve the cold flow characteristics and cetane number of the fuel.<sup>8</sup> The SFC-FID and SFC-MS analysis of these two samples showed no evidence of any polar materials.

The contour plot displayed in Fig. 4 shows that HVO 3 is predominantly comprised of *n*-alkanes, with very few *iso*-alkanes detected, note the streaking shows sample overload. The overloaded sample was used to aid detection and identification of minor components present in the sample. The lack of any significant *iso*-alkane content suggests that the fuel was manufactured with the primary hydrotreatment process only, involving the saturation and removal of the heteroatom content.<sup>5,7,32</sup> This composition could limit the use of HVOs of this type due to a high potential for waxing, *i.e.*, poor cold flow properties. Analysis of the undiluted sample revealed the presence of hexadecanoic acid (C16:0), with other FFAs present at lower concentrations. The identification of each of the species was confirmed using library matching of the EI mass spectra and further confirmed using SFC-FID and SFC-MS using negative ion electrospray ionisation (ESI). Fig. 5 shows the reconstructed ion current chromatograms (RICC) for the deprotonated acids, highlighting the selectivity of this ionisation technique. Further FFAs apart from hexadecanoic acid were detected, including 9-octadecenoic acid (C18:1), *n*-octadecanoic acid (C18:0), 9,12-octadecadienoic acid (C18:2), tetradecanoic acid (C14:0) and dodecanoic acid (C12:0).

One strength of SFC-FID analysis is that it can quantitatively determine the compound class composition of fuels. The analysis involves separation and grouping of each chemical type into simplified elution bands. Fig. 6 is an example of the group separations that highlights the polars, saturates and aromatics elution regions and Table 1 (repeatability data shown in Table S1†) shows the grouping percentages for the seven



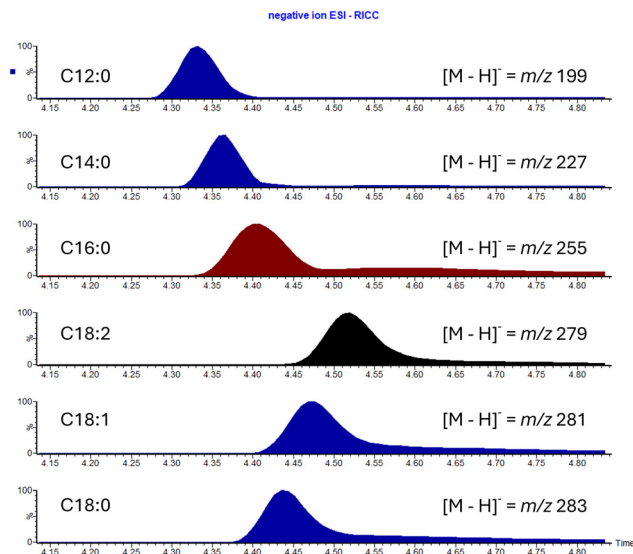


Fig. 5 Reconstructed ion current chromatogram (RICC) of the negative ion ESI SFC-MS of HVO 3.

fuels analysed. The polar region was defined using another standard mixture, data not shown.

GCxGC-MS data also shows group separation information, where a chemical class can be assigned to an area in the two-dimensional chromatogram. In the column configuration used here, the alkanes (*iso*-alkanes and *n*-alkanes) elute first, followed in the second dimension by *cyclo*-alkanes and then the aromatic species. Polar species, typically biofuel related FAMES and FFAs, also elute in a specific region, with assignment of these individual species determined from their EI mass spectra. In this work, the classification was based on a combination of retention time regions and ChromaTOF spectral rule-sets to assign a chemical type. The ruleset contains a set of  $m/z$  values that are characteristic for each of the compound types found in the HVO samples, the class is assigned based on the mass spectra of each of the peaks.<sup>33,34</sup> The alkanes were assigned using a retention times regional-based classification, also available in the software. A simplified representation of where certain classes are expected to elute in the two-dimensional GCxGC-MS data can be found in Fig. 7.

To readily compare different HVO samples, a simple pie chart visualisation approach has been developed and used where the total ion current responses for each of the individual

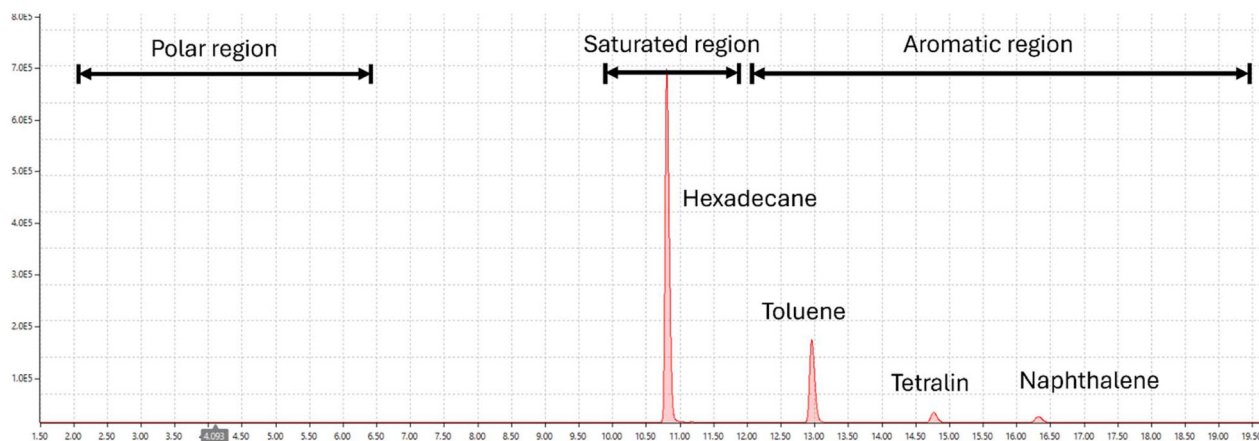


Fig. 6 SFC-FID chromatogram of a standard mix showing group separation regions.

Table 1 The relative response for the HVOs determined by SFC-FID and GCxGC-MS

| HVO sample | Percentage relative response |           |           |                      |           |           |
|------------|------------------------------|-----------|-----------|----------------------|-----------|-----------|
|            | SFC-FID (undiluted) %        |           |           | GCxGC-MS (diluted) % |           |           |
|            | Polar                        | Saturates | Aromatics | Polar                | Saturates | Aromatics |
| 1          | N.D.                         | 100.0     | N.D.      | N.D.                 | 100.0     | N.D.      |
| 2          | N.D.                         | 100.0     | N.D.      | N.D.                 | 100.0     | N.D.      |
| 3          | 1.2                          | 98.4      | 0.4       | 0.7                  | 99.3      | <0.1      |
| 4          | N.D.                         | 96.7      | 3.3       | N.D.                 | 99.0      | 1.0       |
| 5          | <0.1                         | 99.8      | 0.1       | N.D.                 | 98.6      | N.D.      |
| 6          | 1.5                          | 96.2      | 2.3       | 0.4                  | 98.8      | 0.8       |
| 7          | 0.2                          | 98.2      | 1.6       | 0.1                  | 99.7      | 0.2       |

N.D. – Not detected in sample, signal to noise (S/N) less than 3.





Fig. 7 Regions in the GCxGC-MS contour plot where an analyte with a given chemical functionality elute. This is an injection of an undiluted sample to show the lower concentration species present in the HVO 5.

peaks were summed according to their chemical types, e.g., *iso*- or *n*-alkane.

Fig. 8 readily shows that HVO 1 and 2 are very similar in composition, with a high *iso*-alkane to *n*-alkane content. In contrast, HVO 3 is predominantly *n*-alkane in content. The compositions of all the HVOs determined from the GCxGC-MS data aligns well with that obtained for the group classification information achieved using SFC-FID (Table 1). HVO 4 shows an entirely different profile compared to the first three HVOs, see pie charts in Fig. 8. The SFC-FID data of this sample shows a composition that is predominantly saturates (see Fig. S1†), where the unresolved peaks are suggesting different classes of saturated hydrocarbons are present. The GCxGC-MS data re-affirms this and shows a significant fraction of *cyclo*-alkanes present, with their mass spectra identifying these as species ranging from single to four ring systems, including terpanes and steranes, see Fig. 9. The presence of these multi-ring systems suggests that a tall oil feedstock may have been used, a by-product of the wood pulping industry.

The pie chart for HVO 5 shown in Fig. 8 is different again in composition when compared to HVOs discussed previously. It has a large *n*-alkane content, similar to HVO 3, but has a higher *iso*-alkane content, suggesting likely cold flow issues. However, at high concentration polar species are detected by SFC-MS, and SFC-FID indicated that these polars are present at approximately one order of magnitude lower concentration than for HVO 3, see Table 1.

Negative ion ESI SFC-MS of HVO 5 revealed the identity of these polars to be FFAs and based on the mass-to-charge ratios ( $m/z$ ) for the deprotonated molecules, these acids are likely to be C16:0, C18:0 and C18:1 (see Fig. S2†). To observe these species in the GCxGC-MS analysis, undiluted HVO 5 must be used. HVO 6 and HVO 7 also show some unexpected *cyclo*-alkane content, but not at the level observed for HVO 4, see Fig. 8. They also show a similar *iso*- to *n*-alkane ratio, but again



Fig. 8 The average compositions of each of the diluted HVO samples tested, based on three replicates, using the GCxGC-MS. The contribution is based on the total ion current response of each peak in a given chemical class. Repeatability information can be found in Table S2, ESI.†

this is different from other HVOs studied. The presence of the *mono*-cyclic and aromatic content was unexpected if it is assumed that the feedstock was vegetable oils. The presence may be related to processing pathways, in addition to those shown in Fig. 1.<sup>5</sup> The data from the SFC-FID also suggests that the samples were close in compositional make-up, however HVO 7 has a lower polar fraction than HVO 6. This polar content (determined in the SFC-FID data) was identified as FFAs and FAMES using the GCxGC-MS and SFC-MS data sets. The negative ion ESI-MS showed that both samples have ions with  $m/z$  corresponding to C16:0, C18:0, C18:1, C18:2 and C18:3 acids. In the positive ion ESI-MS, both samples had FAMES (of the FFAs as identified in the negative ion ESI) present, with C18:1, C18:2 and C18:3 FAMES, also observed in the GCxGC-MS data. A major difference between HVO 6 and HVO 7 was that TAGs, DAGs and MAGs were detected in the SFC-MS data for HVO 6, see Fig. 10. The presence of these involatile, higher molecular weight compounds may go some way to explain why the GCxGC-MS data under-reports the polar species present when compared to the SFC-FID data.





Fig. 9 GCxGC-MS contour plot (top) and one example of the EI mass spectra and library match spectra of one terpane and one sterane detected in undiluted HVO 4 (bottom).



Fig. 10 Base peak ion current chromatogram (BPIC) of the positive ion ESI SFC-MS for HVO 6.

### Preliminary evaluation of the GCxGC-MS data

The pie charts (Fig. 8) provide a simple approach to visualise similarities and differences between the HVOs. Taking a data-driven approach to explore the results from the other techniques, provides granularity and was used with Table 1 to afford a fuller picture of the HVOs. For example, closer inspection of Table 1 shows good agreement between percentages from the SFC-FID and GCxGC-MS analysis for samples where the composition is mainly saturates (*iso*-alkanes and *n*-alkanes). However, the unexpected presence of polar and/or aromatics shows divergence in the data sets.

Often the GCxGC-MS data under-reports percentages compared to the SFC-FID data, this could be due to differences in volatility of these markedly different materials, *e.g.*, alkanes, *cyclo*-alkanes, aromatics, FFAs and FAMES, where the further the class moves away from the analogous hydrocarbon the greater the difference in melting point/boiling point and ionis-



Fig. 11 Adjusted response based on the compound class of the analytes detected in the GCxGC-MS analysis for HVOs 1 and 6.

ation efficiency would be expected. For example, HVO 1 contains FAMES and TAGs, and preliminary experiments with a standard mixture containing related classes of compounds showed that the FAMES gave approximately half the ionisation response compared to the equivalent alkane (GCxGC-MS data). These TAGs would not be detected by the GCxGC-MS due to these being too involatile, thermally labile and too high a molecular weight.

Fig. 11 shows the pie charts for HVOs 1 and 6, using the assumption of a uniform ionisation response for all components (left) and the adjusted pie charts for the same samples, based on the ionisation efficiency for each class, calculated from use of the standard mixture (right). More detailed work and discussion of these different response factors will be reported in the subsequent publication, where a more granular approach to quantifying the range of materials present will be discussed.

### HVO nomenclature consideration

Critical information required for an HVO is a measure of the *iso*-alkane and *n*-alkane content, the isomerisation of the alkanes is required to address the poor cold flow properties of *n*-alkane rich material. This can be determined using the GCxGC-MS data, *e.g.*, HVO 1 and HVO 2 show near identical profiles for polars, saturates (100%) and aromatics, and the detailed analysis of the *iso*-alkane to *n*-alkane ratios are around 90% *iso*-alkane/10% *n*-alkane and 82% *iso*-alkane/18% *n*-alkane respectively.

Taking HVO 1 as an example, if only the alkane content is considered, then this HVO could be classified as i95 (or i95n5). Since it is 95% *iso*-alkane and 5% *n*-alkane. Similarly, HVO 2 would then be i85 (i85n15) and HVO 3 i1 (i1n99) indicating that this HVO is 99% *n*-alkane.

At this point, it may be worth considering grouping these numerical values into predefined intervals, *i.e.*, bins, see Table 2 where an arbitrary bin size has been used for illustration. The appropriate/useful bin size to be defined by industry.



**Table 2** Suggested bin allocations for the *iso*-alkane content of an HVO

| Bin range (%) | Bin composition | Bin label |
|---------------|-----------------|-----------|
| 0 to 5        | Up to 5%        | i5        |
| 6 to 15       | 15%             | i15       |
| 16 to 25      | 25%             | i25       |
| 26 to 35      | 35%             | i35       |
| 36 to 45      | 45%             | i45       |
| 46 to 55      | 55%             | i55       |
| 56 to 65      | 65%             | i65       |
| 66 to 75      | 75%             | i75       |
| 76 to 85      | 85%             | i85       |
| 86 to 95      | 95%             | i95       |
| 96 to 100     | 100%            | i100      |

Where the total percentage of *iso*- and *n*-alkanes moves away from 100% then these could be reported as follows, *e.g.*, for a hypothetical mix of 60% *iso*-alkane, 25% *n*-alkane and 15% other species, then the ratio of the alkanes may be insufficient, this would round to i70, showing a high degree of isomerisation, i60n25 by default would show that there are other materials present though i60n25o15 would highlight the different composition (i = *iso*-alkane, n = *n*-alkane and o = other material) and could be more useful.

## Conclusions

In this study, orthogonal chromatographic and detection techniques were used to screen different HVO samples and determine their composition, specifically to answer the initial question of whether all HVOs are the same. Primarily, this work revealed that the variation in the different HVOs is linked to the feedstocks used and specific production processes. One unexpected finding was the detection of polar materials within some HVO samples, including FFAs and TAGs, where the presence of these compounds could be detrimental to fuel storage, delivery, and performance. Additionally, each analytical method employed contributed unique insights into the composition of HVOs.

Whilst individual techniques proved useful for identifying specific compounds (that link to fuel properties), only by combining information from the three techniques used can a holistic view of the chemical profile of a fuel be determined. SFC-FID can quantitatively measure the group-based separations (polars, saturates and aromatics) of the different HVOs, without any sample preparation. The extended chromatographic resolution of GCxGC and the power of the mass spectrometer provided identification of the individual fuel components for the saturates and aromatics. Further, the *iso*-alkane to *n*-alkane ratio, a critical factor in assessing cold flow properties, can be quantified. This ratio is particularly important in predicting potential operational challenges, such as fuel performance at lower temperatures. The selectivity of SFC-ESI-MS was able to detect individual polar ionisable compounds (aligned to the polars group separated by the SFC-FID).

This study suggests that “HVO” is too broad a term and does not accurately represent the diverse chemical composition of these fuels. The observed differences between HVOs suggest that further classification into distinct subclasses would be beneficial to reflect these differences between HVOs.

## Author contributions

Laval R. Nicolas: conceptualisation, data curation, investigation, methodology, visualisation, writing – original draft; Jody Clark: resources, methodology; Jim Barker: supervision, resources, writing – review & editing; G. John Langley: supervision, conceptualisation, methodology, writing – review & editing; Julie M. Herniman: supervision, methodology, writing – review & editing.

## Conflicts of interest

There are no conflicts to declare.

## Data availability

Due to number of raw data files acquired during the preparation of this manuscript, the data will be made available upon request.

## Acknowledgements

The authors would like to thank Innospec Limited (Ellesmere Port, UK) for the provision of the HVO samples. In addition, they also thank the University of Southampton, School of Chemistry and Chemical Engineering and Innospec Limited for studentship funding.

## References

- P. Zeman, V. Hönl, M. Kotek, J. Táborský, M. Obergruber, J. Mařík, V. Hartová and M. Pechout, *Catalysts*, 2019, **9**, 337.
- R. Maghrebi, M. Buffi, P. Bondioli and D. Chiaramonti, *Renewable Sustainable Energy Rev.*, 2021, **149**, 111264.
- H. Aatola, M. Larmi, T. Sarjovaara and S. Mikkonen, *SAE Int. J. Engines*, 2008, **1**, 1251–1262.
- S. K. Sikdar and F. Princiotta, *Advances in Carbon Management Technologies: Biomass Utilization, Manufacturing, and Electricity Management*, CRC Press, 2021, vol. 2.
- M. Žula, M. Grilc and B. Likozar, *Chem. Eng. J.*, 2022, **444**, 136564.
- Z. Rahmawati, L. Santoso, A. McCue, N. L. Azua Jamari, S. Y. Ninglasari, T. Gunawan and H. Fansuri, *RSC Adv.*, 2023, **13**, 13698–13714.



- 7 G. W. Huber, P. O'Connor and A. Corma, *Appl. Catal., A*, 2007, **329**, 120–129.
- 8 Y. Aljajan, V. Stytsenko, M. Rubtsova and A. Glotov, *Catalysts*, 2023, **13**, 1363.
- 9 R. M. Smith, *J. Chromatogr., A*, 1999, **856**, 83–115.
- 10 “ASTM Volume 05.05”, American Society of Standards and Materials, 2020, pp. D8305–D8319.
- 11 K. J. Johnson, S. L. Rose-Pehrsson and R. E. Morris, *Energy Fuels*, 2004, **18**, 844–850.
- 12 K. S. KostECKA, A. Rabah and C. F. Palmer Jr., *J. Chem. Educ.*, 1995, **72**, 853.
- 13 R. Pál, M. Juhász and Á. Stumpf, *J. Chromatogr., A*, 1998, **819**, 249–257.
- 14 J. Dallüge, J. Beens and U. A. T. Brinkman, *J. Chromatogr., A*, 2003, **1000**, 69–108.
- 15 P. Vozka, H. Mo, P. Šimáček and G. Kilaz, *Talanta*, 2018, **186**, 140–146.
- 16 R. B. Gaines, G. S. Frysinger, M. S. Hendrick-Smith and J. D. Stuart, *Environ. Sci. Technol.*, 1999, **33**, 2106–2112.
- 17 J. V. Seeley, S. K. Seeley, E. K. Libby and J. D. McCurry, *J. Chromatogr. Sci.*, 2007, **45**, 650–656.
- 18 C. Yang, R. Faragher, Z. Yang, B. Hollebone, B. Fieldhouse, P. Lambert and V. Beaulac, *Fuel*, 2023, **343**, 127948.
- 19 C. Vendeuvre, F. Bertoncini, L. Duval, J.-L. Duplan, D. Thiébaud and M.-C. Hennion, *J. Chromatogr., A*, 2004, **1056**, 155–162.
- 20 M. A. Gough and G. J. Langley, *Rapid Commun. Mass Spectrom.*, 1999, **13**, 227–236.
- 21 C. West, *J. Chromatogr., A*, 2024, **1713**, 464546.
- 22 M. Ashraf-Khorassani, G. Isaac, P. Rainville, K. Fountain and L. T. Taylor, *J. Chromatogr. B: Anal. Technol. Biomed. Life Sci.*, 2015, **997**, 45–55.
- 23 M. Ashraf-Khorassani, J. Yang, P. Rainville, M. D. Jones, K. J. Fountain, G. Isaac and L. T. Taylor, *J. Chromatogr. B: Anal. Technol. Biomed. Life Sci.*, 2015, **983–984**, 94–100.
- 24 P. J. Schoenmakers, J. L. M. M. Oomen, J. Blomberg, W. Genuit and G. Van Velzen, *J. Chromatogr., A*, 2000, **892**, 29–46.
- 25 Food and Agriculture Organization of the United Nations (FAO). Production/Crops and livestock products [Internet]. FOASTAT; 2024 [cited 2025 Jan 30]. Available from: <https://www.fao.org/faostat/en/#data/QCL>.
- 26 T. T. N. Dinh, K. V. To and M. W. Schilling, *Meat Muscle Biol.*, 2021, **5**(1), 34.
- 27 R. C. Zambiasi, R. Przybylski, M. W. Zambiasi and C. B. Mendonça, *Bol. CEPPA*, 2007, **25**(1), 111–120.
- 28 C. Li, Y. Yao, G. Zhao, W. Cheng, H. Liu, C. Liu, Z. Shi, Y. Chen and S. Wang, *J. Agric. Food Chem.*, 2011, **59**, 12493–12498.
- 29 P. Šimáček, D. Kubička, G. Šebor and M. Pospíšil, *Fuel*, 2009, **88**, 456–460.
- 30 B. Veriansyah, J. Y. Han, S. K. Kim, S.-A. Hong, Y. J. Kim, J. S. Lim, Y.-W. Shu, S.-G. Oh and J. Kim, *Fuel*, 2012, **94**, 578–585.
- 31 M. C. Vásquez, E. E. Silva and E. F. Castillo, *Biomass Bioenergy*, 2017, **105**, 197–206.
- 32 R. Tiwari, B. S. Rana, R. Kumar, D. Verma, R. Kumar, R. K. Joshi, M. O. Garg and A. K. Sinha, *Catal. Commun.*, 2011, **12**, 559–562.
- 33 M. K. Jennerwein, M. Eschner, T. Gröger, T. Wilharm and R. Zimmermann, *Energy Fuels*, 2014, **28**, 5670–5681.
- 34 F. W. McLafferty and F. Turecek, *Interpretation of mass spectra*, University Science Books, 4th edn, 1993.

